CARDIORESPIRATORY ABNORMALITIES IN EARLY AND ADVANCED STAGE MOUSE MODELS OF DUCHENNE MUSCULAR DYSTROPHY

A Thesis presented

to the Faculty of the Graduate School

at the University of Missouri-Columbia

In Partial Fulfillment

of the Requirements for the Degree

Master of Sciences

---

by

SUSAN A. OBI

Dr. Maike Krenz, Thesis Supervisor

MAY 2021

The undersigned, appointed by the dean of the Graduate School, have examined the thesis entitled

CARDIORESPIRATORY ABNORMALITIES IN EARLY AND ADVANCED STAGE MOUSE MODELS OF DUCHENNE MUSCULAR DYSTROPHY

presented by Susan A. Obi,

a candidate for the degree of Master of Science,

and hereby certify that, in their opinion, it is worthy of acceptance.

X _____
Dr. Maike Krenz

X _____
Dr. Alan Parrish

X _____
Dr. Timothy Domeier

X _____
Dr. Kevin Cummings

Acknowledgements

I would like to thank my thesis advisor, Dr. Maike Krenz for her unwavering support, keen attention to detail, and for a mentorship relationship that has encouraged question-asking and critical thinking. She has always been readily available to assist and answer questions, has challenged and uplifted me, and has made it possible for me to complete my Master's thesis, even in the midst of unprecedented times. I am gratefully lucky and utterly appreciative to have worked with her.

So too, I would like to thank Dr. Alan Parrish. He has been genuinely supportive and caring throughout my graduate career - from my graduate school application process to graduation, he has always been willing to lend a helping hand and for that I am grateful.

Many thanks to Dr. Domeier for his constant enthusiasm, approachability, and thoughtful insights on this manuscript. I am grateful and honored to have him on my committee.

I would also like to thank Dr. Cummings for his helpful comments and suggestions in writing this manuscript, and for allowing the use of his lab equipment for respiratory experiments.

To my committee, I'm grateful for your assistance; to my fellow lab member, Dr. Lihui Song, I am thankful to have had shared a lab space with you. Your assistance throughout my time in the lab was extremely helpful. Special thanks to my family and friends for your constant love and support. You are all highly appreciated.

TABLE OF CONTENTS

LIST OF ILLUSTRATIONS

Figure Page

LIST OF ABBREVIATIONS

DMD, Duchenne Muscular Dystrophy

GAPDH, Glyceraldehyde 3-phosphate dehydrogenase

WT, Wild-type

kDa, Kilodaltons

ACE, Angiotensin-converting enzyme

PCR, Polymerase Chain Reaction

RV, Right Ventricle

LV, Left Ventricle

V_T, Tidal Volume

V_e, Ventilation

V_e /VCO_2, Ventilatory Equivalent

ABSTRACT

Duchenne muscular dystrophy (DMD) is an X-linked severe muscle disease caused by dystrophin gene mutations affecting 1 in 3,500 newborn males worldwide every year. DMD is characterized by progressive skeletal muscle degeneration and weakness. In advanced disease, respiratory insufficiency and dilated cardiomyopathy limit life expectancy. The purpose of this study was to investigate the time course of myocardial fibrosis and respiratory decline in a mouse model of DMD. The extent of fibrosis was determined in histological sections using planimetry. We found that 16-month-old DMD hearts were in early stages of myocardial fibrosis, with 9.6 +/- 0.04% in the RV (n=3) and 2.1 +/- 0.01% in the LV (n=3). In contrast, the dystrophic changes in the diaphragm at 16 months of age were severe (52.1% fibrosis). Using whole-body plethysmography and pulse oximetry, we assessed respiratory function and blood oxygen saturation (SaO_2). At 12 months of age, Dmd*mdx*^{4cv} mice exhibited significantly lower respiratory frequency and oxygen consumption. However, ventilation (V_e) and ventilatory equivalent (V_e/VCO_2) were not different compared to wild-type littermates, in part due to slightly increased tidal volume. Likewise, there was no effect of genotype on SaO_2. These data suggest that while the dystrophic changes in the diaphragm were severe, overall respiratory status is not severely compromised in 12–16-month-old DMD mice. Altogether, these data provide a framework for determining the time course of cardiorespiratory decline in DMD mice. In the future, this could lead to new therapeutic approaches to minimize DMD-induced heart and respiratory failure at early-stage disease.

INTRODUCTION

Dystrophin

The dystrophin gene is the largest known human gene. It contains 2.6 million DNA base pairs and 79 exons, making up roughly 0.1% of the entire genome (4) (6). This gene is located in the short arm of the X chromosome and is responsible for supplying instructions for production of the dystrophin protein. Dystrophin is a large, rod-shaped cytoplasmic protein consisting of four domains: actin-binding amino-terminal domain, a central rod domain, a cysteine-rich domain, and a carboxyl-terminus (4). The size of this protein is 427kDa. Due to its large size, dystrophin is prone to high rates of spontaneous mutation (11). Dystrophin is a vital part of the muscle cell membrane as it acts as an anchor linking the actin cytoskeleton to the muscle cell membrane via the dystroglycan complex. The dystroglycan complex is composed of an alpha subunit (α-dystroglycan) and a beta subunit (β-dystroglycan) as shown in green in **Figure 1** (α-DG and β-DG).

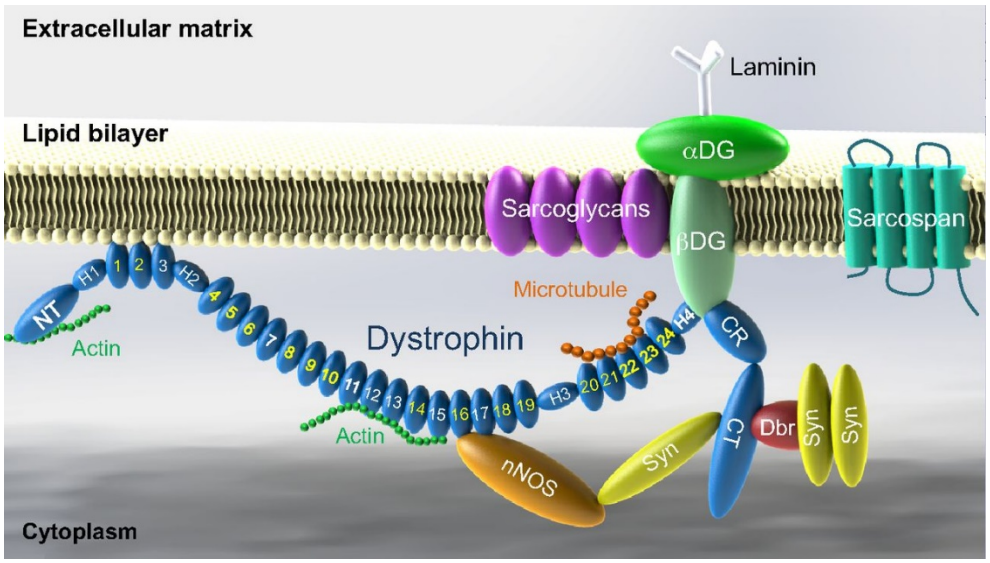

Figure 1. Schematic outline of the dystrophin protein anchored to the actin cytoskeleton and the dystroglycan complex. Dystrophin consists of the actin-binding amino-terminal domain (N-terminus), a central rod domain (consisting of 24 spectrin-like repeats), a cysteine-rich domain (CR) and a carboxyl-terminus (CT) (10).

Dystrophin is necessary to maintain the integrity of the sarcolemma (5). If the skeletal muscle contracts in the absence of dystrophin or presence of a truncated dystrophin protein, the muscle cell membrane will weaken overtime and eventually tear. This provides a pathway, allowing ions such as calcium to leak into the cell. Elevated levels of intracellular calcium will activate proteases leading to damage of fully functional proteins and myocyte death. Due to plasma membrane leakiness, creatine kinase (CK) levels in the blood will increase. High blood levels of CK are a known marker for Duchenne muscular dystrophy (DMD). This eventually leads to fibrosis as the lost myocytes will be replaced with fat and scar tissue.

Duchenne Muscular Dystrophy

Muscular dystrophies (MDs) are a group of inherited diseases characterized by progressive muscle weakness and skeletal muscle wasting. Every year, 1 in 3,500 newborn males worldwide are affected by this devastating disease (4). There are multiple forms of MDs including congenital MD, distal MD, myotonic MD, Becker muscular dystrophy and Duchenne muscular dystrophy with DMD being the most common (7).

DMD is characterized by progressive muscle weakness due to mutations in the dystrophin gene. Point mutations are the most common form of mutations in DMD (4). This occurs when a single base pair in a gene is altered. This can either be categorized as a missense or nonsense mutation. A missense mutation is one in which a nucleotide substitution leads to a change in the encoded amino acid. A nonsense mutation occurs when the nucleotide substitution leads to generation of a stop codon, ultimately leading to a truncated protein.

DMD is inherited as an X-linked recessive trait, therefore, primarily affecting males since males only possess one X chromosome. Females may also inherit a mutated gene which would cause them to be carriers of this disease. About 8% of female carriers display a DMD phenotype (39). The mutations in the dystrophin gene lead to loss of dystrophin protein in both skeletal and cardiac muscle, resulting in progressive weakness, skeletal muscle wasting, and reduced ability of the heart to pump blood.

The first historical account of DMD occurred in the first half of the 19th century (8)(9). Dr. Charles Bell, an English physician described the symptoms of an 18-year-old boy who was experiencing partial muscle paralysis:

“” All *the muscles of the lower extremities, the hips, and the abdomen, are debilitated and wasted…. He has no defect of sensibility in the lower extremities. The upper part of the body, the shoulders, and arms, are strong. There is no defect perceptible in the evacuation of the bladder or of the bowels…. The paralytic debility of the muscles came on gradually; he was first sensible of it at a public school, about eight years ago. It began with a weakness in the thighs, which disabled him from rising; and it is now curious how he will twist and jerk his body to throw himself upright from his seat*. (4)””

Subsequently, Italian physicians documented similar cases of two brothers with their main symptoms being progressive muscle weakness and pseudohypertrophy in the upper and lower extremities. Prevalence of these cases began to increase in the 1850s. French neurologist Guillaume Duchenne closely examined 13 cases of males with muscle weakness, bulging muscles and difficulty walking. He concluded that these patients were experiencing more than just mere progressive muscle weakness and “spinal” muscle atrophy as was originally thought (8).

Progressive Symptoms

Clinical symptoms of DMD occur as early as 3 years of age and include difficulties in walking and changing body position. Patients will also exhibit a phenomenon known as Gowers' sign which was observed by neurologist Sir William Richard Gowers in 1879 (12). This occurs when DMD patients place their hands on their knees to support themselves in rising from a supine position due to weakness of hip and knee extensors (12). The Gower's sign is commonly used as a screening test for DMD.

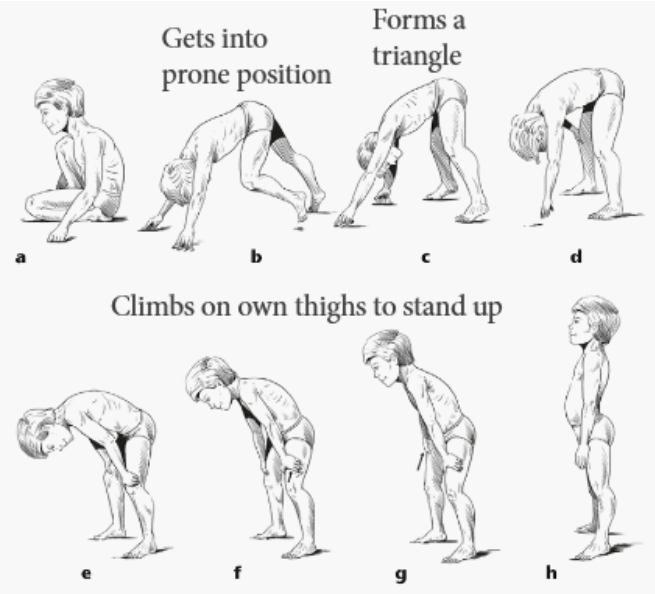

Figure 2. Male DMD patient exhibits Gower's sign. *"He helps himself up in a very peculiar way—by putting his hands upon his knees, and grasping his thighs higher and higher, and so by…climbing up his thighs he pushes his trunk up.*"(13). **(a)** Patient resting in a kneeling position, most likely occurring after being in supine position. **(b)** Patient gets into prone position. **(c)** Patient forms a triangle shape while pushing against the floor to support himself. **(d)** Patient continues to attempt rising to a standing position. **(e)** Patient now begins to support himself by placing his hands against his knees. **(f-g)** patient progressively moves his hands upward from his knees to his thighs. **(h)** Patient with arched back while standing upright.

Due to progressive muscle weakness, patients will ultimately become wheelchair-dependent. Because the diaphragm is a muscle, it is unfortunately affected by DMD and patients will eventually require respiratory assistance. In end-stage disease, the symptoms include severe heart failure as the life-limiting effect. It is important to note that neurological defects are not the cause of muscle weakness and instability as may be seen in spinal cord injuries or progressive muscle atrophy (8).

According to the National Institute of Health (NIH), and the Genetic and Rare Diseases Information Center (GARD), 80-99% of DMD patients experience these symptoms: calf muscle hypertrophy, cardiomyopathy, cognitive impairment, delayed speech and language development, elevated serum CK, scoliosis, skeletal muscle atrophy, progressive muscle weakness and respiratory insufficiency (14) (23).

Cardiovascular Effects of DMD

Severe heart failure is the most common cause of death in DMD patients, more specifically, progressive dilated cardiomyopathy (2). In end-stage disease, chronic hypoxia often occurs leading to pulmonary hypertension (26), which substantially increases workload of the right ventricle. Previous studies have indicated that the initial stages of heart failure may begin in the right ventricle (RV) (25).

The function of the heart is to pump oxygenated blood throughout the body. Deoxygenated blood flows from the superior vena cava to the right atrium of the heart, through the tricuspid valve to the right ventricle. From the right ventricle, blood is pumped to the lungs through the pulmonary valve. In the lungs, deoxygenated blood becomes oxygenated as gas is being exchanged between the alveoli and the capillaries - oxygen diffuses from the lungs into the bloodstream while carbon dioxide diffuses from the bloodstream into the lungs. When the oxygenated blood leaves the lungs, it flows from the left atrium to the left ventricle via the mitral valve. It is then pumped from the left ventricle to the aorta via the aortic valve. The aorta then distributes blood to the body's tissues.

Patients with DMD typically present with cardiac fibrosis and early diastolic dysfunction between the age of 10 and 15 (18) (19). Because the heart muscle becomes progressively weaker over time, the heart is not able to efficiently pump oxygenated blood to the tissues. This eventually progresses to cardiomyopathy as the life-limiting effect.

Due to little understanding concerning pathophysiology of DMD induced heart failure, there are limited therapeutic options. This includes ACE inhibitors and corticosteroids (2). These drugs are effective in slowing down disease progression, although unfortunately cannot abolish the detrimental effects. As a result, the average age of mortality in DMD patients can begin as early as mid to late 20s (20).

Respiratory Function in DMD

In DMD patients, respiratory insufficiency usually occurs during the non-ambulatory stage. This is because DMD patients who have become wheelchair dependent often suffer from scoliosis which may affect the chest cavity structure and compliance due to the abnormal spine curvature (24). Symptoms of breathing difficulties in DMD include shallow breathing, hypoventilation, wheezing, weakened cough, difficulty sleeping, shortness of breath, and severe oxygen desaturation. (15) (24).

The diaphragm is a voluntary and involuntary muscle located under the lungs and is affected by DMD. Its function is to assist with breathing, more specifically, inhalation. When the diaphragm contracts, it moves downward, thus increasing the volume in the thoracic cavity, which causes the pressure round the lungs to decrease, pulling the lung open. Subsequently, the increased volume in the lungs lead to a decrease in pressure which causes oxygen to move from the atmosphere into the lungs upon inhalation. There are additional muscles that assist with increasing the space in the thoracic cavity, these are known as accessory muscles. The accessory muscles include but are not limited to the scalenes, sternocleidomastoid, and the latissimus dorsi. These muscles function to elevate the upper and lower ribs, and to elevate the sternum respectively (28). Since all patients with DMD experience respiratory muscle weakness (15), the diaphragm and accessory muscles eventually weaken, leading to decreased space in the thoracic cavity. As a result, the lungs are not able to expand

sufficiently, thus gas exchange is slowed, resulting in hypoventilation, eventually leading to hypercapnia and decreased oxygen intake. It is important to note that the lungs of DMD patients are not directly affected by this disease. Rather, it is the diaphragm that is directly affected as it is a skeletal muscle. This in turn affects the lungs leading to respiratory insufficiency in early-stage disease.

Mouse Models of DMD

To more closely study and understand the pathophysiology of DMD, it is important to have an animal model that is closely analogous to the human disease of DMD and develops a vast majority of the effects that are seen in DMD patients. Without a viable animal model, it will be difficult to understand DMD as seen in humans, and to lay the groundwork for suitable therapeutic approaches. The mdx mouse model was used more frequently in the past and contains a nonsense mutation at exon 23 that ultimately leads to loss of the dystrophin protein; however, it does not develop the DMD dilated cardiomyopathy and does not have a shortened lifespan (1). The skeletal muscle displays mild/moderate changes in histopathology and function, and age of onset for the mdx mouse model is about 3-4 weeks. While the histopathology of the cardiac muscle is mild, mdx mice display little to no dysfunction (1). The age of onset for the cardiac muscle is about 10 months (1).

There are various other DMD mouse models such as *mdx*^{2cv}, *mdx*^{3cv}, *mdx*^{4cv}, and *mdx*^{5cv} which were created from the C57BL/6 mouse strain (1).

These mouse models were created by treating mice with a chemical mutagen, N-ethyl-*N*-nitrosourea, and each of these models contain different types of mutations. The *mdx*^{2cv} and *mdx*^{3cv} mouse models contain a point mutation at the splice acceptor of intron 42 and intron 65 respectively, while the *mdx*^{4cv} and *mdx*^{5cv} contain a point mutation at exon 53 and exon 10 respectively (1). This results in a premature stop codon in the *mdx*^{4cv} mouse model as the point mutation is a nonsense mutation. The Dmd*mdx*^{4cv} mouse model is a strain of the mdx mouse and is often used as it exhibits disease effects as seen in humans. A potential reason for this may be that this model has 10-fold fewer revertants compared to other models. Since the Dmd*mdx*^{4cv} mouse is not able to replace lost skeletal muscle fibers, due to its fewer revertants, this is an advantage to study the effects of DMD in the skeletal muscle during early-stage disease. Our rationale for using the Dmd*mdx*^{4cv} mouse model was to detect subtle pathological changes that occur in DMD mice and to note the time course of progression for cardiac and skeletal muscle fibrosis.

OBJECTIVES

The purpose of this study was to note the time course of cardiopulmonary insufficiencies in DMD mice. To do this, we assessed cardiac fibrosis and respiratory function in Dmd*mdx*^{4cv} mice that varied in age. Using this mouse model of DMD, we investigated the subtle pathological dystrophic changes that occur in the cardiac muscle of younger, compared to older Dmd*mdx*^{4cv} mice. We also assessed fibrosis in the diaphragm of older Dmd*mdx*^{4cv} mice and evaluated

their respiratory function. Respiratory function was also determined in very young mice in order to note the time course of respiratory insufficiency in the Dmd*mdx*^{4cv} mouse model and for comparison to studies in the literature.

HYPOTHESIS

Significant dystrophic changes in the cardiac and diaphragm muscle will be detected in the older mice and will be more severe in the older Dmd*mdx*^{4cv} mice than in the younger Dmd*mdx*^{4cv} mice. Moreover, the respiratory function of older, but not younger Dmd*mdx*^{4cv} mice will be severely compromised.

MATERIALS AND METHODS

Experimental Animals

The animals used for this study were male Dmd*mdx*^{4cv} mice. There were two age ranges used for this study: young (2–6-month-old mice) and older (12-16- month-old mice). The young mice were in the early stages of DMD while the older mice were in advanced stage disease. Animals were housed in animal care facilities of the University of Missouri. All experiments involving mice were approved by the University of Missouri Animal Care & Use Committee and conducted in accordance with the *American Physiological Society Guiding Principles in the Care and Use of Vertebrate Animals in Research and Training*. C57BL/6J and B6Ros.Cg- Dmd*mdx*^{4cv} /J (mdx^{4cv}) mice were purchased from The Jackson Laboratory (*stock numbers 000664 and 002378*). Heterozygous mice were generated in house by crossing C57BL6/J with mdx^{4cv}. For all experiments, the controls used were wild type littermates of the Dmd*mdx*^{4cv} mice.

PCR Genotyping Based on Primer Competition. There were three primers used for mdx genotyping: a common reverse primer (DL1579), a wild type allele-specific forward primer (DL1532) and a mutant allele-specific forward primer (DL1575). Tail DNA was extracted using phenol / chloroform followed by alcohol precipitation. The PCR condition was set as (1) an initial denaturation at 95°C for 2 min; (2) five cycles of the first stage amplification including 95°C denaturation for 20 sec, 62°C annealing for 20 sec, and 72°C extension for 20 sec; (3) 23 cycles of the second stage amplification, and (4) a final extension at 72°C for 1 min. The PCR was performed in a Bio-Rad thermal cycler. The PCR products were resolved in a 3% agarose gel (27).

Protein Analyses. For total protein extracts, flash-frozen mouse ventricles were homogenized in lysis buffer [150 mM NaCl, 10 mM Tris (pH 7.4), 1% Triton X-100, and 1x HALT Protease & Phosphatase Inhibitor Cocktail (Sigma-Aldrich)]. The homogenates were centrifuged (8,000 g for 10 minutes at 4°C). Protein concentrations in the supernatant were determined colorimetrically using a dye-binding assay (Bio-Rad). After boiling, proteins were separated by SDS-PAGE (10% acrylamide gels) and transferred to polyvinylidene difluoride membranes (Bio-Rad). Membranes were blocked with TBS-T and nonfat milk (5%). The following primary antibodies were used for Western blotting: Monoclonal (MANDYS1(3B7)) and Glyceraldehyde 3-Phosphate Dehydrogenase (GAPDH) (D16H11) XP® (1:1000) from Cell Signaling Technologies. Primary antibody binding was visualized by horseradish peroxidase-conjugated secondary

antibodies and enhanced chemiluminescence (Amersham; GE Healthcare) using a Bio-Rad ChemDoc imaging system.

Histological Analysis. For cardioplegic arrest in end-diastole, mice underwent deep inhalation anesthesia using 2–3% isoflurane with 0.6 liters flow of O_2. Hearts were perfused through the apex with 4% paraformaldehyde in phosphate-buffered saline containing 25 mM KCl and 5% dextrose. Hearts were then further fixed with 4% paraformaldehyde in phosphate-buffered saline overnight, infused with 30% sucrose, embedded in Tissue-Tek OCT compound, frozen, and cut into 7-micrometer cryosections. Longitudinal sections through the middle of the heart where leaflets of both mitral and tricuspid valves were seen in the same plane were stained with Hematoxylin and Eosin (Sigma-Aldrich) and Gomori's One-Step Trichrome (Poly Scientific) according to manufacturers' specifications.

Image Analysis/Planimetry. Images were obtained using an Olympus BX60 Microscope and Cellsens software. NIH Image J was used to perform image analysis.

Plethysmography. Data were recorded from unrestrained animals kept within a water-perfused glass plethysmographic chamber (volume: 100ml) maintained at an ambient temperature of 27°C. Air (21% O_2, balance N_2) from a gas cylinder passed through a flowmeter prior to entering the chamber via a 20G needle pushed through one of the rubber stoppers that seal the chamber. Chamber pressure was kept near atmospheric by pulling the gas from the opposite end of

the chamber with the pump from a O_2/CO_2 analyzer (model GA-200, iWorx Systems, Inc., Dover, NH), also through a 20G needle. Air flow through the chamber was held constant at 250 ml/min. The analog signal from the respiratory pressure transducer was fed into a Powerlab data acquisition system (ADInstruments) and analyzed in LabChart V8 (ADInstruments).

Pulse oximetry. The MouseOx Plus was used for this experiment and contains multiple sensors available to monitor or record measurements on both conscious and anesthetized mice, rats, and other small animals. Blood oxygen saturation and heart rate were measured using a collar sensor that obtains a signal from the carotid arteries. This sensor measures changes of light absorption in oxygenated and deoxygenated blood.

Statistical Analysis. All data are expressed as mean +/- S.D. (S.E.M.). For all data sets, comparisons between Dmdmdx^{4cv} mice and control littermates were evaluated using Student's unpaired t-test, and $p < 0.05$ was considered statistically significant.

RESULTS

Mdx^{4cv} genotyping

To more closely study and understand the pathophysiology of DMD, we used the Dmd*mdx*^{4cv} mouse model. Mutant allele specific primer and Wild-Type allele specific primer were used in mdx^{4cv} genotyping. These primers were in competition to bind with the mouse dystrophin gene; the expected sizes were 141 base pairs for the wild-type product and 123 base pairs for the mdx^{4cv} product. The PCR products are shown in **Fig. 3**.

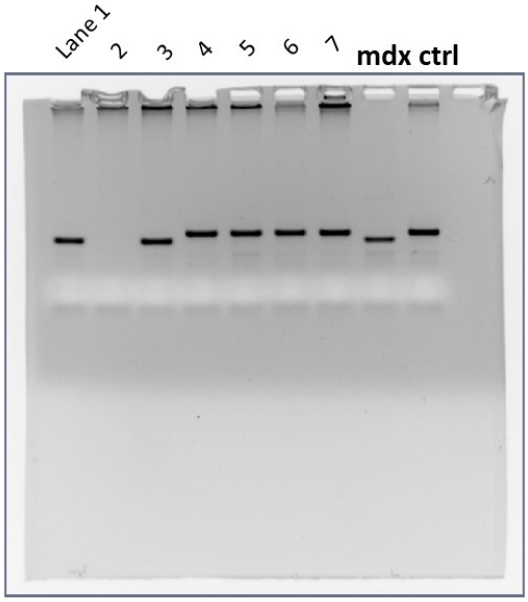

Figure 3. Quantitative PCR results for mdx^{4cv} genotyping. Bands in lanes 4-7 are representative of control mice. Bands in lanes 1 and 3 are representative of Dmd*mdx*^{4cv} mice.

Protein Analyses

To evaluate the dystrophin expression in the mice, Western blot analysis was used to quantify dystrophin expression in ventricular tissue from wild-type (WT) and Dmd*mdx*^{4cv} mice. Western blot analysis of samples from WT and Dmd*mdx*^{4cv} mice is shown in **Fig. 4**. In Dmd*mdx*^{4cv} samples (lanes 3, 5-7, and 11), no dystrophin can be detected. In contrast, samples from WT mice (lanes 1-2, 4, and 8-10) show normal levels of dystrophin. This confirms that the nonsense mutation in Dmd*mdx*^{4cv} mice results in loss of dystrophin protein.

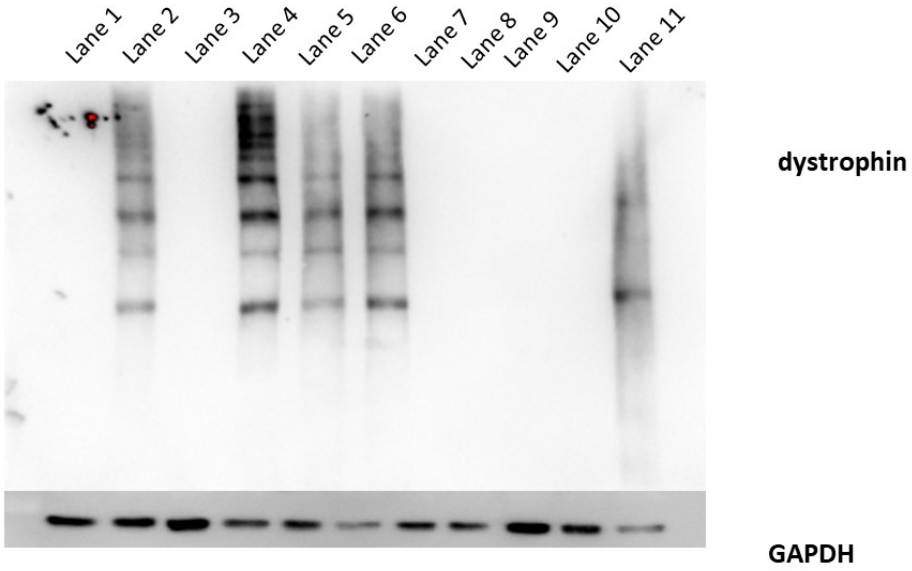

Figure 4. Protein analysis for WT and Dmd*mdx*^{4cv} mice. Western blot analysis indicates lack of dystrophin expression in Dmd*mdx*^{4cv} mice (upper panel). Lanes 3, 5-7 and 11 are representative of the Dmd*mdx*^{4cv} mice. Lanes 1-2 and 4 are representative of the WT mice. GAPDH was used as loading control (lower panel).

Dystrophic Changes in Cardiac Muscle (six-month-old mice)

To determine the extent of cardiac fibrosis in a young, six-month-old Dmd*mdx*^{4cv} mice, histological analyses using Gomori Trichrome staining were performed. The amount of fibrosis was determined via planimetry in both six-month-old WT mice and six-month-old Dmd*mdx*^{4cv} mice. In the following figure, data are shown as percentage of fibrotic area for the right ventricular free wall (**Fig. 5**), the left ventricle (left ventricular free wall and septum, **Fig. 6**), and as total percentage for both ventricles combined (**Fig. 7**). There was not a significant difference in right ventricular fibrosis between the WT mice and DMD mice (**Fig. 5B-C**). We also determined the extent of fibrosis in the LV (**Fig. 6A**) and again saw no significant differences between WT and Dmd*mdx*^{4cv} mice.

In summary, we discovered that there was a negligible amount of myocardial fibrosis in both the RV and the LV, and there was no significant difference in the total myocardial fibrosis between the two groups (**Fig. 7**). Overall, these data suggests that the Dmd*mdx*^{4cv} mice hearts are not severely fibrotic at six months of age, exhibiting less than 2% total fibrosis.

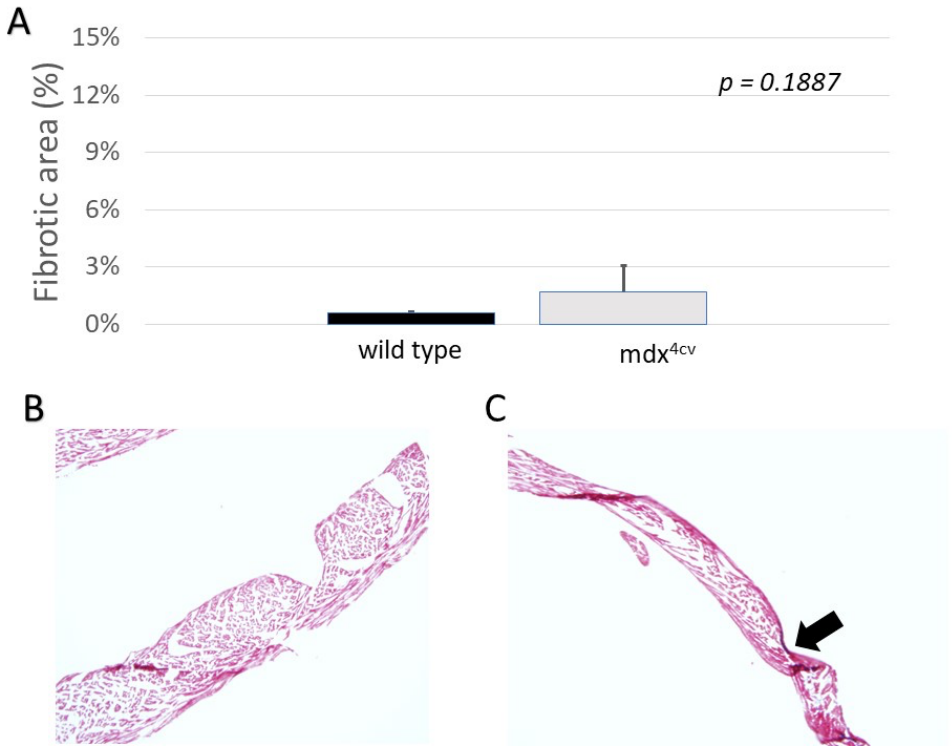

Figure 5. Myocardial collagen expression and fibrosis in right ventricle of wild-type (WT) and Dmdmdx^{4cv} mice. (A) Percentage of fibrotic areas in the right ventricle (RV) of six-month-old wild type mice (n=3) and six-month-old Dmd*mdx*^{4cv} mice (n=6). The percent of fibrosis is indicated by the black bars for WT mice and the gray bars for Dmd*mdx*^{4cv} mice. **(B)** Representative section of RV in wild type mice stained with Gomori Trichrome. **(C)** Section of RV in DMD mice stained with Gomori Trichrome. Fibrotic areas are shown by the black arrows. P value < 0.05 was considered statistically significant.

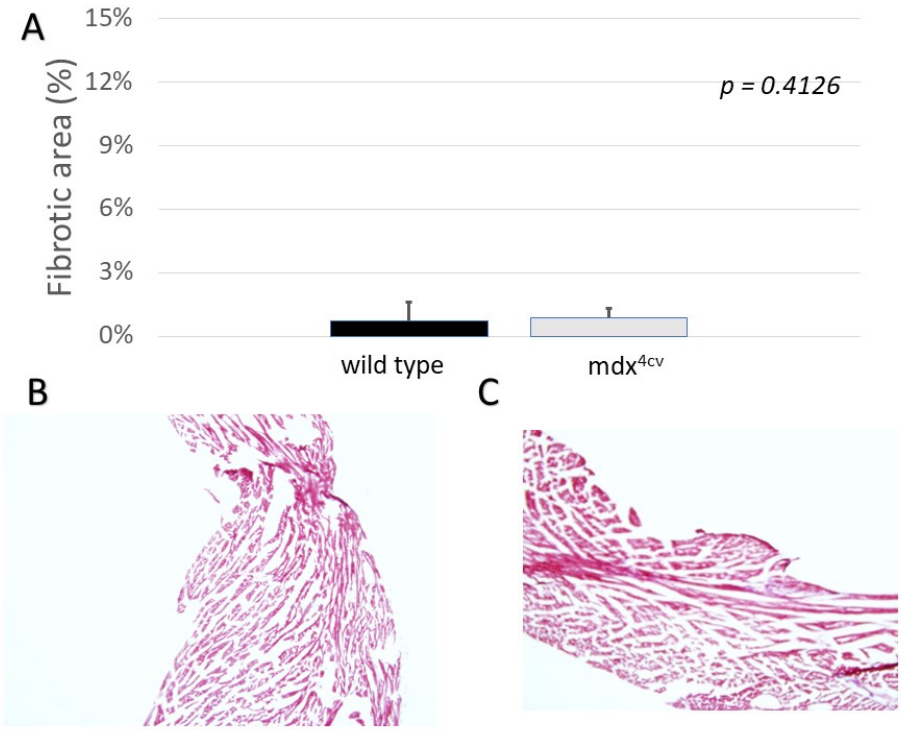

Figure 6. Fibrosis in left ventricle of wild-type (WT) and Dmd*mdx*^{4cv} mice. **(A)** Percentage of fibrotic areas in the left ventricle of six-month-old wild type mice (n=3) and six-month-old DMD mice (n=6). The percent of fibrosis is represented by the black bars for WT and the gray bars for mdx^{4cv}. **(B)** Section of LV in six-month-old wild type mice stained with Gomori Trichrome. **(C)** Section of LV in six-month-old DMD mice stained with Gomori Trichrome. P value < 0.05 was considered statistically significant.

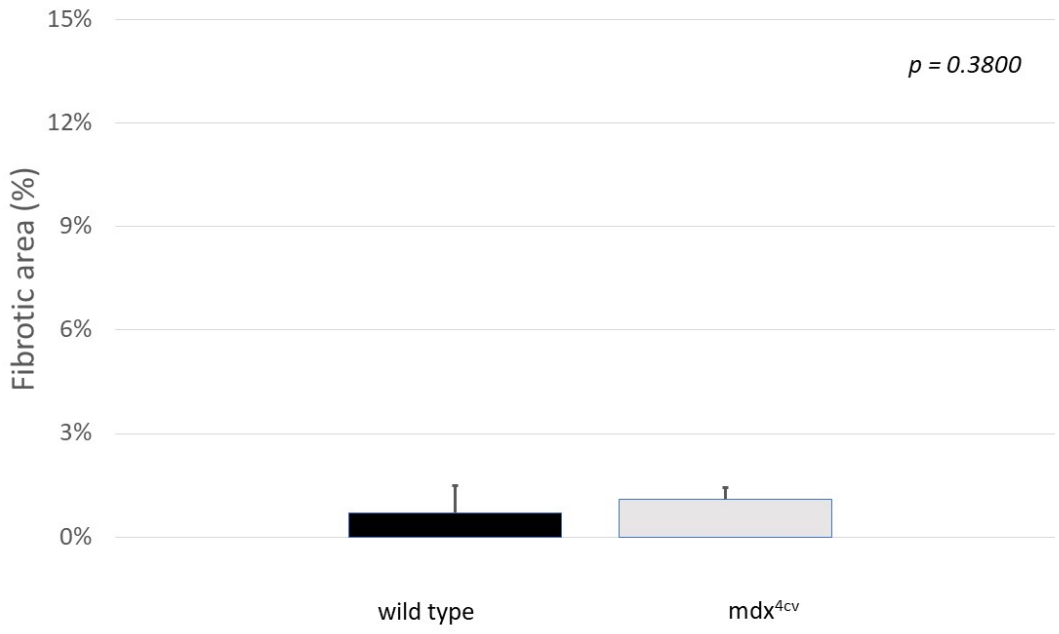

Figure 7. Total myocardial collagen expression and fibrosis in WT mice and Dmd*mdx*^{4cv} mice. Expression of total myocardial fibrosis in six-month-old WT mice (n=3) and Dmd*mdx*^{4cv} mice (n=6). The percent of fibrosis is shown by the black bars for WT and the gray bars for mdx. P value < 0.05 was considered statistically significant.

Dystrophic Changes in Cardiac Muscle (16-month-old mice)

Next, we assessed the extent of cardiac fibrosis in older DMD mice at 16 months of age. Using Gomori Trichrome staining, we found that there was a trend towards increased right ventricular fibrosis in the same-aged Dmd*mdx*^{4cv} mice compared to the WT mice, but this trend did not reach statistical significance (**Fig. 8**). Similarly, there were no significant differences in LV (**Fig. 9**) or total fibrosis (**Fig. 10**), although trends to higher levels of fibrosis were observed **(Fig. 10**).

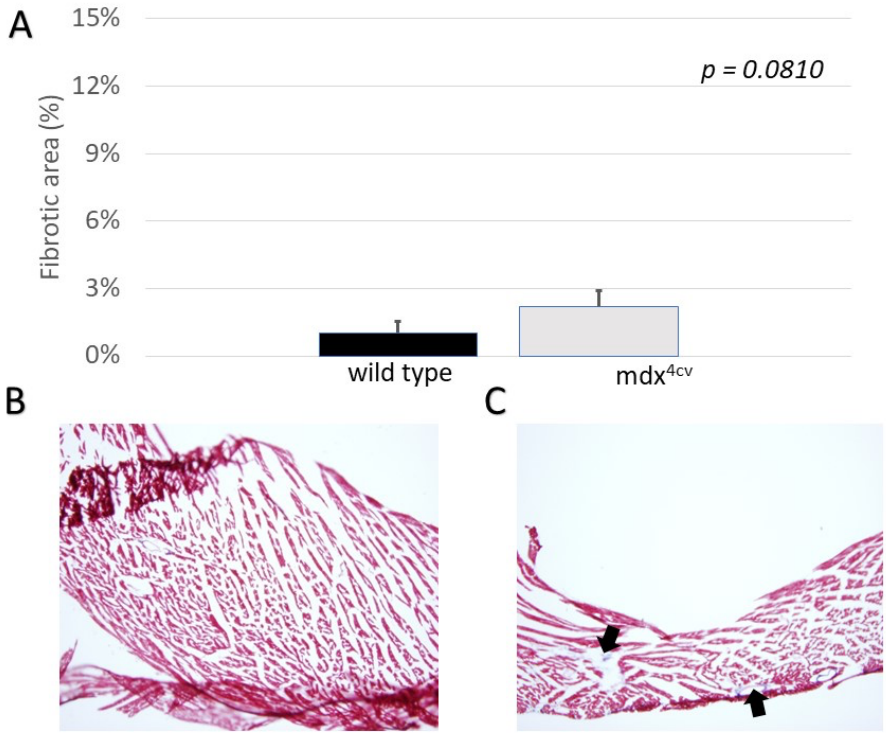

Figure 8. Fibrosis in right ventricle of wild-type (WT) and Dmd*mdx*^{4cv} mice. **(A)** Percentage of fibrotic areas in the right ventricle of sixteen-month-old wild type mice and sixteen-month-old DMD mice respectively. The percent of fibrosis is represented by the black bars for WT (n=3) and the gray bars for mdx^{4cv} (n=3). **(B)** Section of RV in sixteen-month-old wild type mice stained with Gomori Trichrome. **(C)** Section of RV in sixteen-month-old DMD mice stained with Gomori Trichrome. Fibrotic areas are indicated by the black arrows. P value < 0.05 was considered statistically significant.

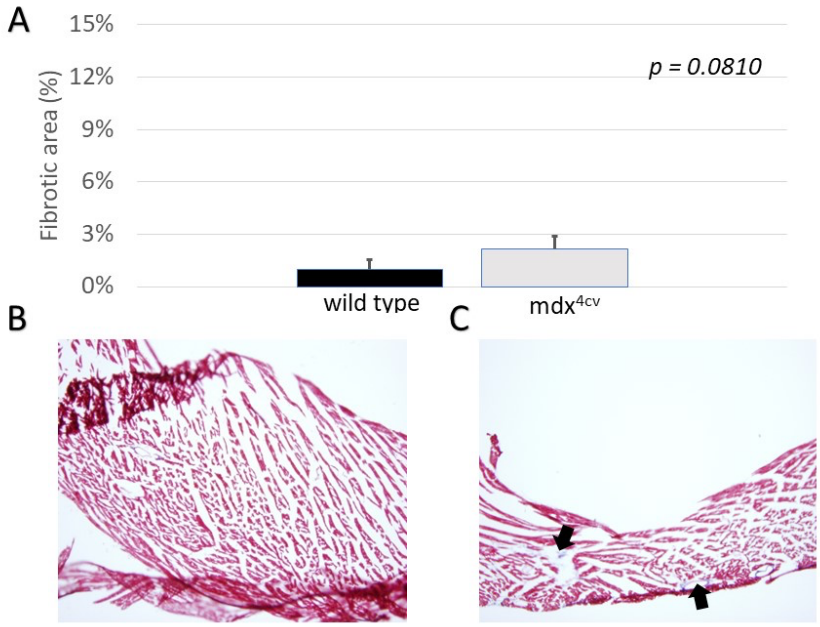

Figure 9. Myocardial collagen expression and fibrosis in left ventricle of wild-type (WT) and Dmd*mdx*^{4cv} mice. (A) Percentage of fibrotic areas in the left ventricle of sixteen-month-old WT mice (n=3) and sixteen-month-old DMD mice (n=3). **(B)** Section of LV in sixteen-month-old WT mice stained with Gomori Trichrome. **(C)** Section of LV in sixteen-month-old DMD mice stained with Gomori Trichrome. P value < 0.05 was considered statistically significant. Fibrotic areas are indicated by the black arrows.

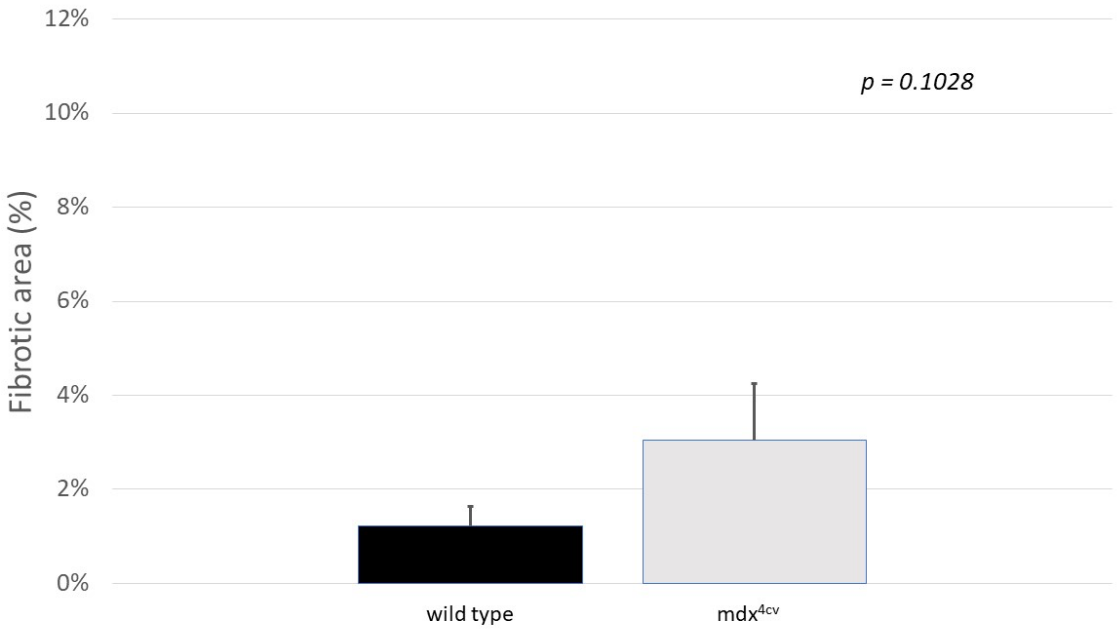

Figure 10. Total myocardial collagen expression and fibrosis in WT mice and Dmd*mdx*^{4cv} mice. Total myocardial fibrosis in sixteen-month-old WT mice (n=3) and Dmd*mdx*^{4cv} mice (n=3). P value of 0.05 was considered statistically significant.

Dystrophic Changes in Diaphragm Muscle (16-month-old mice)

As we found surprisingly low levels of cardiac fibrosis in 16-month-old Dmd*mdx*^{4cv} mice, we decided to also assess the extent of diaphragm fibrosis in 16-month-old Dmd*mdx*^{4cv} mice compared to WT mice. This was determined in Gomori Trichrome-stained histological sections using planimetry. The diaphragm of the 16-month-old WT mice showed a negligible amount of fibrosis under the microscope **(Fig. 11A)**, while the Dmd*mdx*^{4cv} mouse diaphragm was severely fibrotic (**Fig. 11B**). There was a significant difference in dystrophic changes seen in the WT mice diaphragm compared to the Dmd*mdx*^{4cv} mice **(Fig. 11C).** Surprisingly, the diaphragm of the Dmd*mdx*^{4cv} mice exhibited an alarming amount of fibrosis compared to the cardiac muscle of the 16-month-old Dmd*mdx*^{4cv} mice **(Fig. 11D)**. These data indicate that: 1) The diaphragm muscle is severely affected in the DMD mice at 16 months of age. 2) The diaphragm muscle is more severely affected than the cardiac muscle in 16-month-old Dmd*mdx*^{4cv} mice.

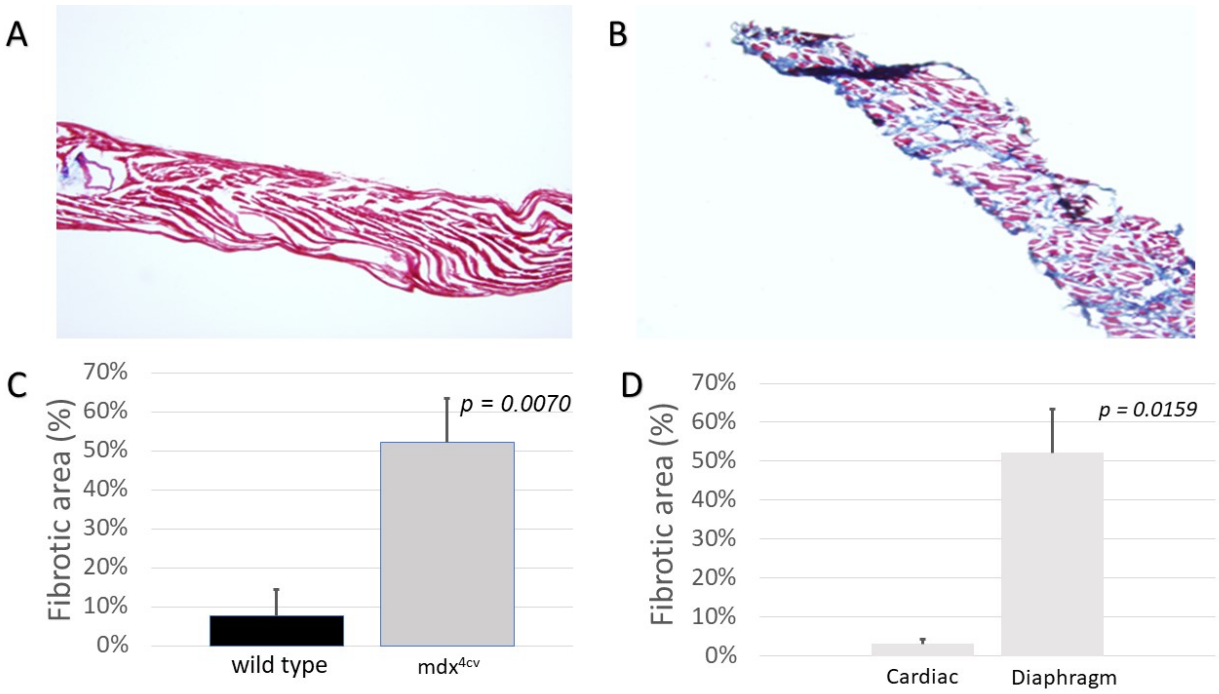

Figure 11. Gomori staining of the diaphragm in 16-month-old mice. **(A)** Section of diaphragm in 16-month-old WT mice. Gomori Trichrome staining was used to detect fibrosis **(B)** Section of diaphragm in 16-month-old Dmd*mdx*^{4cv} mice. **(C)** Total fibrotic area in diaphragm of WT mice (n=3) as represented by the black bar scale and Dmd*mdx*^{4cv} mice (n=3) as represented by the gray bar scale. **(D)** Total percent of fibrosis in 16-month-old DMD mice cardiac muscle and diaphragm muscle respectively. P value < 0.05 is considered statistically significant.

Evaluation of Respiratory Function in Advanced Stage Dmd*mdx*^{4cv} mice (12 months old)

The diaphragm muscle of the 16-month-old Dmd*mdx*^{4cv} mice showed increased amount of fibrosis compared to the cardiac muscle **(Fig. 11D).** Based on these findings, we tested whether respiratory function of advanced stage Dmd*mdx*^{4cv} mice would be impaired. Whole body plethysmography and pulse oximetry were used on 12-month-old Dmd*mdx*^{4cv} mice to evaluate respiratory function. We measured variables such as respiratory frequency (f), tidal volume (V_T), ventilation (V_E), oxygen consumption (VO_2), metabolic CO_2 production (VCO_2) and the ventilatory equivalent (V_E/VCO_2; an index of blood gas status) of both wild-type and Dmd*mdx*^{4cv} mice. Pulse oximetry was used to measure blood oxygen saturation (SaO_2) in mice during and just after anesthesia. As mentioned previously, we hypothesized that overall respiratory function would be compromised in 12-month-old Dmd*mdx*^{4cv} mice.

Respiratory Frequency and Tidal Volume in Advanced Stage Dmd*mdx*^{4cv} mice

Whole body plethysmography, which measures changes in volume of air in the lungs, was used to determine respiratory frequency in WT and Dmd*mdx*^{4cv} mice. Respiratory frequency is defined as breaths per minute (bpm). We also determined tidal volume which is expressed in ml/min and is defined as the volume of air delivered to the lungs with each breath. Respiratory frequency was significantly lower in Dmd*mdx*^{4cv} mice compared to WT mice **(Fig. 12A).**

Interestingly, there was a trend for higher tidal volume in the mdx mice compared to the WT mice **(Fig. 12B**). A reason for this may be that the mice were compensating for lower respiratory frequency by increasing their tidal volume.

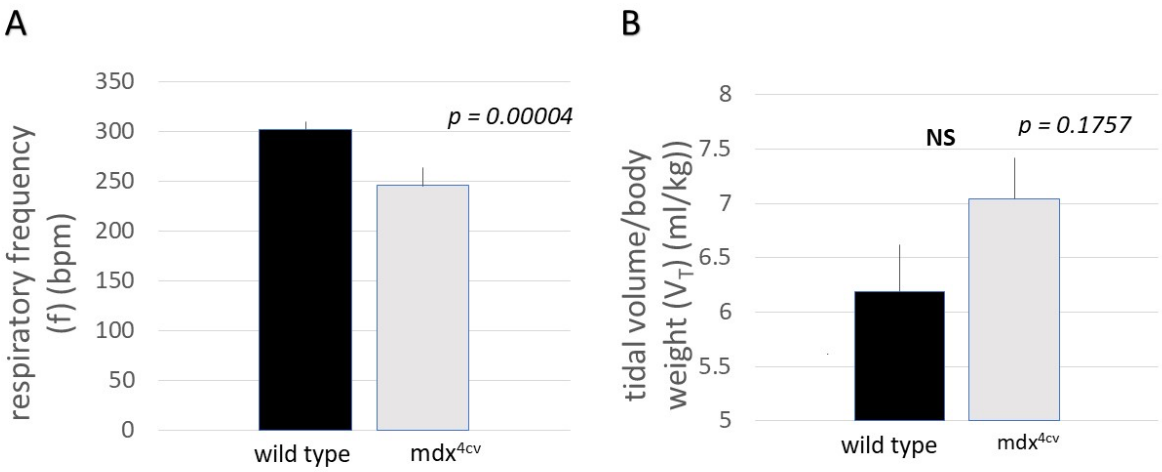

Figure 12. Respiratory frequency and tidal volume in 12-month-old wild type mice and Dmd*mdx^{4cv}* mice. Bar graphs were used to show variations between respiratory parameters. **(A)** Respiratory frequency (f) of 12-month-old WT mice and 12-month-old DMD mice. **(B)** Tidal volume (V_T). The *f* and V_T of WT mice (n =8) is indicated by the black bar. The gray bar indicates the f and V_T of the mdx^{4cv} mice (n=9).

Respiratory Function Variables in Advanced Stage Dmd*mdx^{4cv}* mice

Ventilation is defined as frequency x tidal volume – the air flowing into the lungs during inspiration (inhalation) and out of the lungs during expiration (exhalation). There was no significant difference in ventilation when wild type mice were compared to Dmd*mdx^{4cv}* mice **(Fig. 13A).** This suggests similar breathing patterns between the two genotypes. Ventilatory equivalent (V_e /VCO_2) was also measured in WT and Dmd*mdx^{4cv}* mice. V_e /VCO_2 is described as the volume of gas expired per minute to the volume of CO_2 consumed per minute and is an indicator of blood gases. There was no significant difference in V_e /VCO_2 when wild type mice were compared to Dmd*mdx^{4cv}* mice **(Fig. 13B)**. This suggests that there is not significant difference in blood gases between WT and Dmd*mdx^{4cv}* mice. Metabolic responses such as oxygen consumption (VO_2) and metabolic CO_2 production were also measured in WT and Dmd*mdx^{4cv}* mice for comparison. VO_2 is defined as the volume of oxygen taken in by the body per minute. Metabolic CO_2 production was also measured (VCO_2). VCO_2 is defined in ml/min, this is the volume of carbon dioxide produced per minute and is an index of basal metabolic rate. Oxygen consumption and carbon dioxide output were significantly lower in Dmd*mdx^{4cv}* mice compared to WT mice **(Fig. 13 C-D).**

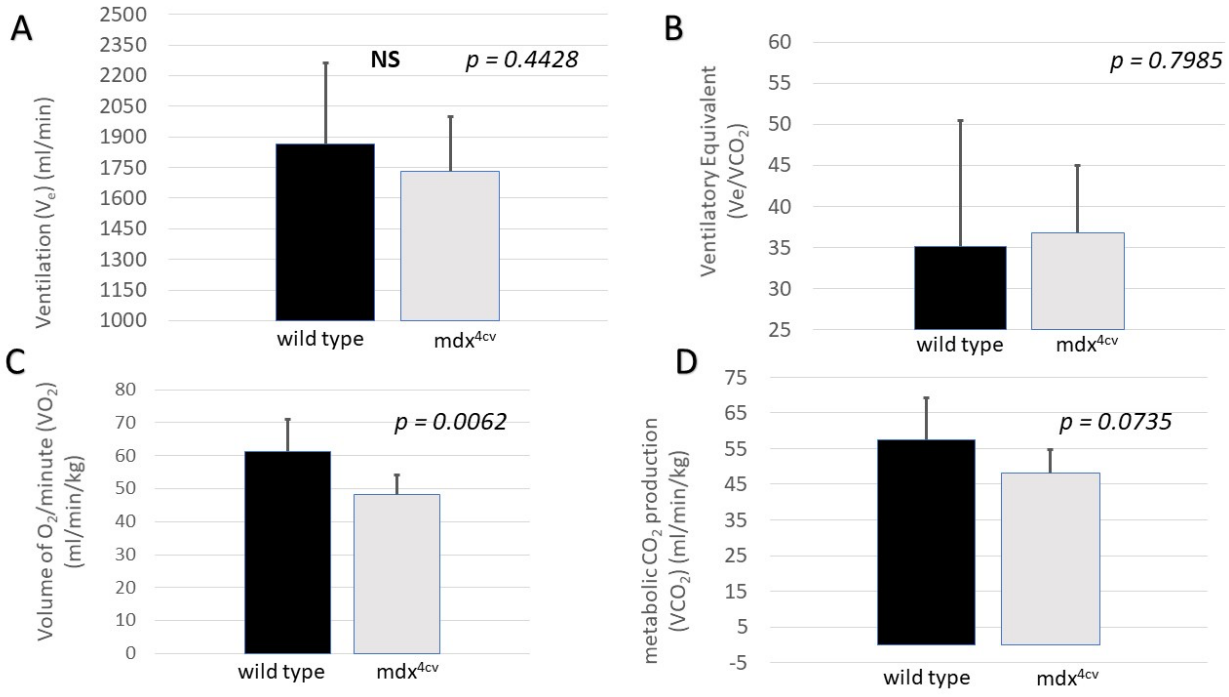

Figure 13. V_e, V_e /VCO_2, VO_2 and VCO_2 in WT and Dmd*mdx^{4cv}* mice. (A) Ventilation, **(B)** Ventilatory Equivalent, **(C)** VO_2, **(D)** VCO_2. The respiratory variables of WT mice (n =8) are indicated by the black bar. The gray bar indicates the f and V_T of the mdx^{4cv} mice (n=9)

Oxygen Saturation in WT and Dmd*mdx*^{4cv} mice

Oxygen saturation is the percent of hemoglobin bound to oxygen. This is indicative of the blood gas status. There was no significant difference in O_2 saturation between WT and Dmd*mdx*^{4cv} mice whether anesthetized or conscious. This suggests that gas exchange is unchanged between the two genotypes.

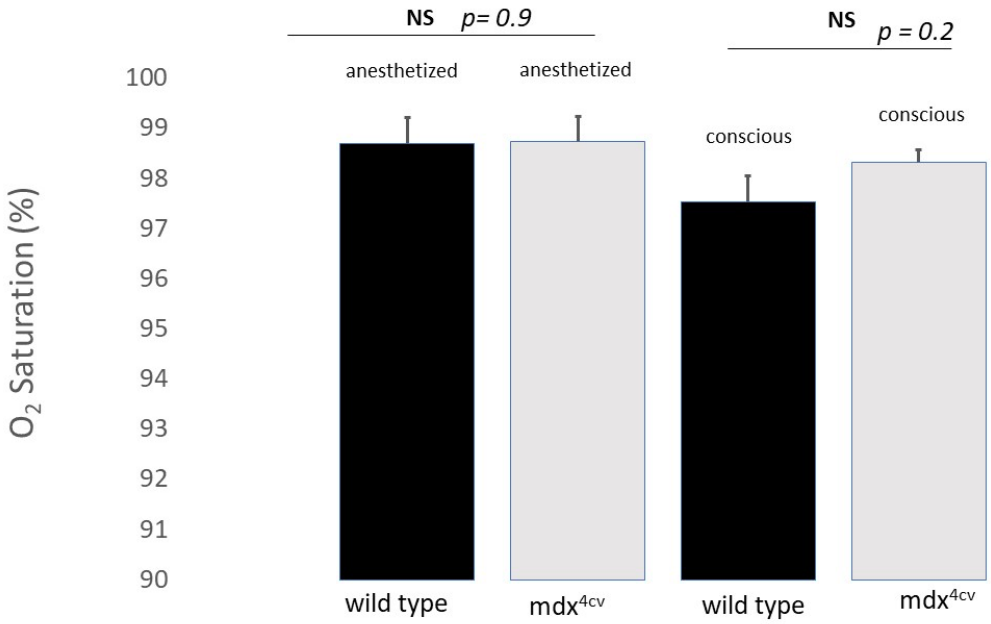

Figure 14. Oxygen saturation in 12-month-old WT and Dmd*mdx*^{4cv} mice during and just after anesthesia. The oxygen saturation of WT mice (n =8) is indicated by the black bar. The gray bar indicates the f and V_T of the mdx^{4cv} mice (n=9).

In conclusion, Dmd*mdx*^{4cv} mice had a significantly lower respiratory frequency than wild type mice. Tidal volume in wild type and Dmd*mdx*^{4cv} mice were not significantly different, but there was a trend for higher V_T in Dmd*mdx*^{4cv} mice. Dmd*mdx*^{4cv} mice may be compensating for low respiratory frequency by

increasing their tidal volume. There was no significant difference in ventilation between wild type mice and Dmd*mdx*^{4cv} mice, nor was there a significant difference in ventilatory equivalent between wild type mice and Dmd*mdx*^{4cv} mice. Since Dmd*mdx*^{4cv} mice may be compensating for their lower frequency, we did not expect to see a change in ventilation between the two groups. Moreover, oxygen consumption and carbon dioxide output were significantly lower in Dmd*mdx*^{4cv} mice compared to wild type mice, but oxygen saturation between wild type mice and Dmd*mdx*^{4cv} mice was not significantly different. The lower metabolic rate of the Dmd*mdx*^{4cv} mice is a notable finding and may in part be attributed to less physical activity in the Dmd*mdx*^{4cv} mice. The similarities in oxygen saturation between the two groups suggests that blood gases are the same, and that gas exchange is not compromised in the diseased mice. Altogether, these data suggest that while metabolic rate is lower in Dmd*mdx*^{4cv} mice, respiratory status in 12-month-old Dmd*mdx*^{4cv} mice is not severely compromised. Also, the Dmd*mdx*^{4cv} mice may use breathing compensatory mechanisms in response to lower respiratory frequency.

Evaluation of Respiratory Function in Young Dmd*mdx*^{4cv} mice (8 weeks old)

Respiratory function was also determined in very young mice for comparison to studies in the literature, whole body plethysmography was used on 8-week-old Dmd*mdx*^{4cv} mice. We measured variables such as respiratory frequency (f), tidal volume (V_T), ventilation (V_E), oxygen consumption (VO_2), metabolic CO_2 production (VCO_2) and the ventilatory equivalent (V_E/VCO_2; an

index of blood gas status) of both wild-type and Dmd*mdx*^{4cv} mice. We hypothesized that overall respiratory function would not be compromised in 8-week-old Dmd*mdx*^{4cv} mice, and that there would not be a significant difference in respiratory sufficiency in the 8-week-old Dmd*mdx*^{4cv} mice compared to their littermates.

Respiratory Frequency and Tidal Volume in Young Dmd*mdx*^{4cv} mice

The same procedures used to measure respiratory frequency in 12-month-old mice was also used in the 8-week-old mice. We found that respiratory frequency or tidal volume was not significantly different in Dmd*mdx*^{4cv} mice compared to WT mice **(Fig. 15A-B).**

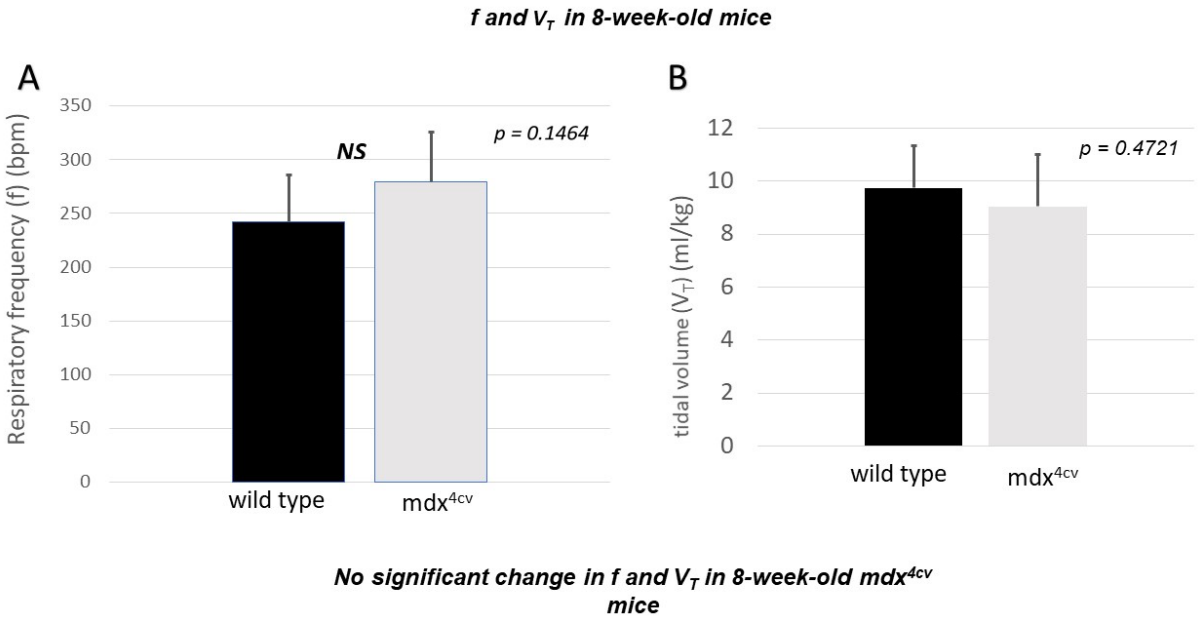

Figure 15. Respiratory frequency and tidal volume in 8-week-old wild type mice and Dmd*mdx^{4cv}* mice. Bar graphs were used to show respiratory parameters. **(A)** Respiratory frequency (f) of 8-week-old WT mice and 8-week-old Dmd*mdx^{4cv}* mice. **(B)** Tidal volume (V_T). The *f and V_T* of WT mice is indicated by the black bar. The *f and V_T* of Dmd*mdx^{4cv}* mice is indicated by the gray bar.

Respiratory Function Variables in Younger Dmd*mdx^{4cv}* mice

The same respiratory variables were measured in the 8-week-old DMD mice, ventilation (V_E), oxygen consumption (VO_2), metabolic CO_2 production (VCO_2), and the ventilatory equivalent (V_E/VCO_2; an index of blood gas status). We also measured oxygen saturation (SaO_2). There was no significant difference in ventilation when wild type mice were compared to Dmd*mdx^{4cv}* mice **(Fig. 16A).** This suggests similar breathing patterns between the two genotypes. Ventilatory equivalent (V_e /VCO_2) was also measured in WT and DMD mice and is an indicator of blood gases. There was no significant difference in V_e /VCO_2 when

WT mice were compared to Dmd*mdx*^{4cv} mice **(Fig. 16B)**. This suggests that there is not significant difference in blood gases between the two groups. Metabolic responses such as oxygen consumption (VO_2) and metabolic VCO_2 production were also measured in WT and DMD mice for comparison. We found that there was no significant difference in metabolic responses in Dmd*mdx*^{4cv} mice compared to WT mice **(Fig. 16 C-D).**

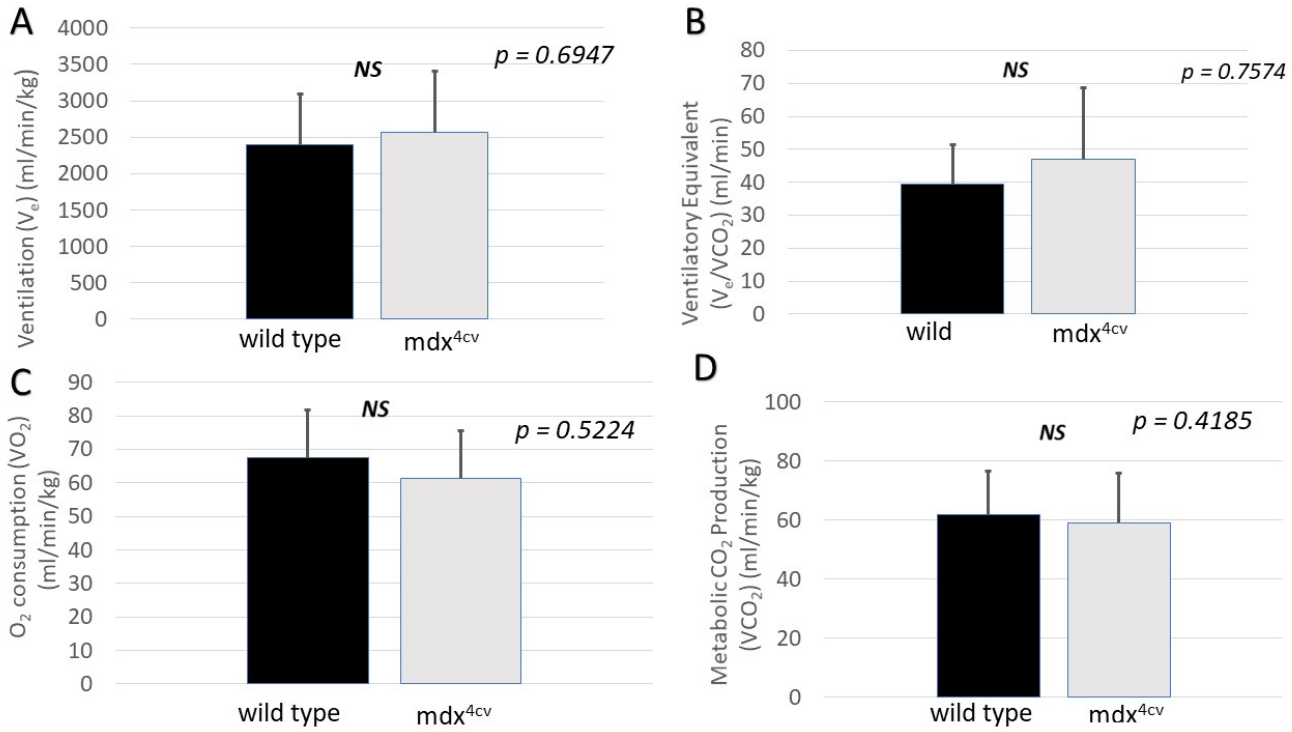

Figure 16. V_e, V_e /VCO_2, VO_2 and VCO_2 in WT and Dmd*mdx*^{4cv} mice. Bar graphs were used to show respiratory parameters. **(A)** Ventilation (V_e) of 8-week-old WT mice and 8-week-old Dmd*mdx*^{4cv} mice, **(B)** Ventilatory Equivalent (V_e /VCO_2), **(C)** Oxygen consumption (VO_2), **(D)** Metabolic CO_2 Production (VCO_2).

In conclusion, respiratory frequency, and tidal volume between the 8-week-old Dmd*mdx*^{4cv} mice and the 8-week-old wild type mice were not

significantly different. Also, oxygen consumption and carbon dioxide output were not different between the two groups. There was no significant difference in ventilation between 8-week-old WT mice and 8-week-old Dmd*mdx*^{4cv} mice, nor was there a significant difference in ventilatory equivalent and oxygen saturation between wild type mice and Dmd*mdx*^{4cv} mice. This suggests that blood gases were the same. Overall, these data suggest that respiratory status in 8-week-old DMD mice is not severely compromised, and that there is no significant difference in respiratory function between the 8-week-old Dmd*mdx*^{4cv} mice and the 8-week-old WT mice.

.

DISCUSSION

Duchenne Muscular Dystrophy (DMD) is the most common form of muscular dystrophy; affecting 1 in 3,500 males per year and 1 in 5,000 males worldwide (31). While there is not a cure for this disease, there are several therapeutic options to mitigate the effects of DMD. The effectiveness of the current therapies is attributable to advancing research in the area of muscular dystrophy. In order to further understand the pathophysiology of DMD, we used a Dmd*mdx*^{4cv} mouse model to more intimately study this disease and to detect subtle pathological changes. The purpose of this study was to assess cardiac fibrosis and respiratory function in Dmd*mdx*^{4cv} mice with aging. Histological analysis of WT and Dmd*mdx*^{4cv} mouse hearts was performed. To determine lung function, whole body plethysmography was used to measure respiratory variables, while pulse oximetry was used to measure oxygen saturation. We hypothesized that significant dystrophic changes in the cardiac and diaphragm muscle will be detected in the older mice, and will be more severe in the older Dmd*mdx*^{4cv} mice than in the younger Dmd*mdx*^{4cv} mice. Moreover, the respiratory function of older, but not younger Dmd*mdx*^{4cv} mice will be severely compromised.

The main findings of this study were: (1) Six-month-old Dmd*mdx*^{4cv} mice showed little cardiac fibrosis (1.2% total) compared to the 16-month-old Dmd*mdx*^{4cv} mice that showed 3.12% total myocardial fibrosis. (2) The diaphragm of the older DMD mice (16 months old) was severely compromised with 52.1% total fibrosis. (3) Interestingly, there was a significant difference in percent of

fibrosis that was seen in the diaphragm of the 16-month-old Dmd*mdx*^{4cv} mice compared to the cardiac muscle of same-aged mice. (4) The respiratory function of the older Dmd*mdx*^{4cv} mice (12 months old) was not severely compromised, and the mice showed probable compensatory mechanisms for breathing. (5) There was no significant difference in respiratory function of the young WT mice and the young Dmd*mdx*^{4cv} mice (8 weeks old).

In the six-month-old mouse model of DMD, we assessed RV fibrosis, LV fibrosis, and total myocardial fibrosis. Using the Gomori Trichrome staining method, the blue dye stained for collagen, which was indicative of fibrosis. At six months of age, there was not a significant difference in the histopathology of the cardiac myocytes in the WT mice and Dmd*mdx*^{4cv} mice. The age of onset in the cardiac phenotype of the mdx mouse is at 10 months (1). Because there is little difference in the clinical presentation of mdx mice compared to mdx^{4cv} mice (10), we expected the age of onset in the mdx^{4cv} mice to be fairly similar. In addition, we also assessed cardiac fibrosis in the 16-month-old mice and found that the Dmd*mdx*^{4cv} mice displayed a increased dystrophic phenotype compared to the WT mice that were the same age. Furthermore, the total myocardial fibrosis in the 16-month-old DMD mice was significantly increased compared to the 6-month-old DMD mice; this trend was seen in both the RV and LV. Previous studies found similar results in myocardial fibrosis of 17-month-old DMD mouse hearts. They reported about 9% fibrosis in the RV wall, and roughly 7% fibrosis in the anterior wall (regions of the LV) (32).

Because the loss of dystrophin protein affects the skeletal muscle, this alters the phenotype of the diaphragm, leading to difficulties in breathing. Previous studies have reported changes in the passive properties of the diaphragm muscle due to loss of dystrophin. Stephens and Faulkner *et al*., 2000 report that an increase in strain of the diaphragm muscle in mdx mice leads to greater stress compared to the control mice. Strain is referring to the % of L_W. L_W is the length at which maximum work is achieved under standard conditions (35). They state that a ~10% increase in strain in the mdx mice was associated with a 40% decrease in power and a 50% increase in stress, while the control mice had a 16% decrease in power and no stress was generated. In addition, Burns *et al*., 2017 reported a significantly reduced twitch force in mdx diaphragm muscle preparations compared to the WT mice. Moreover, at 8 weeks of age, the force frequency relationship in mdx diaphragm preparations was significantly reduced compared to the WT mice. We assessed the total fibrosis in the diaphragm of Dmd*mdx*^{4cv} mice at 16 months of age and found that the diaphragm displayed a severely fibrotic phenotype, and interestingly, was drastically more fibrotic than the cardiac muscle of the same-aged Dmd*mdx*^{4cv} mice. Given that the 16-month-old Dmd*mdx*^{4cv} mice presented with a little over 50% fibrosis in the diaphragm, we expected to see a substantial change in their respiratory function. This led us to test for several respiratory parameters such as respiratory frequency (f), tidal volume (V_T), ventilation (V_E), oxygen consumption (VO_2), metabolic CO_2 production (VCO_2) and the ventilatory equivalent (V_E/VCO_2) of both wild-type and Dmd*mdx*^{4cv} mice in order to compare and contrast between the two genotypes.

Because of limited available resources, we used 12-month-old Dmd*mdx*^{4cv} mice for this study and expected that the respiratory status would be comparable in 12–16-month-old Dmd*mdx*^{4cv} mice. Conscious whole-body plethysmography (WBP) was used to determine respiratory parameters as it detects pressure changes associated with breathing.

We found that the 12-month-old Dmd*mdx*^{4cv} mice had significantly lower breaths per minute (bpm) compared to the WT mice, however, there was a trend for higher tidal volume in the Dmd*mdx*^{4cv} mice. Furthermore, there was no significant difference in ventilation between WT mice and Dmd*mdx*^{4cv} mice. Ventilatory equivalent and oxygen saturation between WT mice and Dmd*mdx*^{4cv} mice were also unchanged, suggesting that blood gases are the same between the two groups at 12 months of age.

These results suggest compensatory breathing mechanisms in the Dmd*mdx*^{4cv} mice. A decrease in respiratory frequency (bpm) indicates that Dmd*mdx*^{4cv} mice are not breathing as often as the WT mice, thus, an increase in the volume of air brought into the airways and lungs with each breath would compensate for decrease in bpm, thereby maintaining ventilation. Ishizaki *et al.* 2008 (34) reported that at 7 months of age, mdx mice had a significantly higher respiratory rate and a significantly lower tidal volume when compared to WT mice. This also suggests a compensatory mechanism of breathing at 7 months of age, albeit a different “strategy” (higher frequency to compensate for lower tidal volume).

Studies have shown that 8-week-old mdx mice already begin to show respiratory decline in tidal volume, thus leading to decreased ventilation as respiratory frequency stays the same (29, 30). In order to note the time course of respiratory insufficiency in the Dmd*mdx*^{4cv} mouse model and to compare to studies in the literature, we used WBP to measure the same respiratory parameters on young Dmd*mdx*^{4cv} mice that were 8 weeks of age. We found no significant differences in f, V_T, V_E, and the ventilatory equivalent V_E/VCO_2 between wild-type and Dmd*mdx*^{4cv} mice. Furthermore, VO_2 and VCO_2 remained unchanged between the two genotypes.

Burns *et al*., 2017 reported a significantly lower tidal volume and ventilatory equivalent in mdx mice compared to WT mice at 8 weeks of age. There are a couple factors to note when considering the difference in the mentioned findings and the findings in our study: 1) The sample size used for our study was n = 8, while the sample size used for the previously mentioned study (Burns *et al*., 2017) was n = 12. This may slightly contribute to apparent differences in tidal volume. 2) The mouse model used in the previously mentioned study is the mdx mouse model. As mentioned earlier, this mouse model seemingly has an increased number of revertants compared to the Dmd*mdx*^{4cv} mouse model. Although we were not able to measure diaphragm fibrosis in 8-week-old mice, another study (Hoffman *et al*. 2015) found that at 8 weeks of age, there is 11.04%±2.3 collagen content seen in the diaphragm, which is indicative of fibrosis. Moreover, the same study reports 41.48%±6.6 centrally nucleated myofibers, which are indicative of myofiber regeneration. It is

important to note that the mdx mice do not exhibit a similar pathogenic progression as seen in human DMD patients. The large increase of centrally nucleated myofibers is used as a marker for DMD progression in the mdx mice, and the regeneration of these myofibers has a rapid occurrence in the first six weeks after birth. This regeneration may largely contribute to differences seen in the respiratory function of mdx mice compared to Dmd*mdx*^{4cv} mice.

In addition, in a subsequent study, Burns *et al*., 2019 reported no significant changes in respiratory frequency (P = 0.2114) and tidal volume (P= 0.4171) between WT and mdx mice at 8 weeks of age (37). Both Mosqueira *et al.* 2013 and Ishizakin *et al.* 2008 show reduced breathing frequency in mdx mice. These findings, together with findings in our study suggests a defect in the respiratory rhythm generating regions in the brain in Dmd*mdx*^{4cv} mice. Dystrophin is expressed in neurons (36), and as mentioned previously, there is other evidence of CNS abnormalities associated with DMD (14)(23). The possibility of defects in the central control of breathing is unclear and should be investigated in the future.

Future Directions

The purpose of this study was to note the time course of cardiopulmonary abnormalities in Dmd*mdx*^{4cv} mice. Future directions of this study could include performing echocardiography on the young and advanced stage Dmdmdx^{4cv} mice. Also, testing for diaphragm fibrosis in 8-week-old mice would prove useful for determining the extent of respiratory insufficiencies and its contribution to respiratory function. As the central control of breathing in DMD remains unclear,

studies investigating the role of dystrophin in the neurons and its implications in altered respiratory function would be beneficial in understanding more clearly the pathophysiology of respiratory dysfunction in DMD.

BIBLIOGRAPHY

1. Yucel, Nora, Alex C. Chang, John W. Day, Nadia Rosenthal, and Helen M. Blau. “Humanizing the Mdx Mouse Model of DMD: The Long and the Short of It.” *Npj Regenerative Medicine* 3, no. 1 (February 16, 2018): 4.
2. Chun, Ju Lan, Robert O’Brien, and Suzanne E. Berry. “Cardiac Dysfunction and Pathology in the Dystrophin and Utrophin-Deficient Mouse during Development of Dilated Cardiomyopathy” 22, no. 4 (April 1, 2012): 368–79.
3. Chun, Ju Lan, Robert O’Brien, and Suzanne E. Berry. “Cardiac Dysfunction and Pathology in the Dystrophin and Utrophin-Deficient Mouse during Development of Dilated Cardiomyopathy” 22, no. 4 (April 1, 2012): 368–79. https://doi.org/10.1016/j.nmd.2011.07.003.
4. Gao, Quan Q, and Elizabeth M McNally. “The Dystrophin Complex: Structure, Function, and Implications for Therapy.” *Comprehensive Physiology* vol. 5,3 (2015): 1223-39.
5. Porter, G A et al. “Dystrophin colocalizes with beta-spectrin in distinct subsarcolemmal domains in mammalian skeletal muscle.” *The Journal of cell biology* vol. 117,5 (1992): 997-1005.
6. Nowak, Kristen J, and Kay E Davies. “Duchenne muscular dystrophy and dystrophin: pathogenesis and opportunities for treatment.” *EMBO reports* vol. 5,9 (2004): 872-6.

7. National Institute of Health. “Muscular Dystrophy: Hope Through Research | National Institute of Neurological Disorders and Stroke.” *National Institute of Health*, NIH Publication No. 13-77, Aug. 2013
8. Tyler, Kenneth L. “Origins and early descriptions of "Duchenne muscular dystrophy".” *Muscle & nerve* vol. 28,4 (2003): 402-22. doi:10.1002/mus.10435
9. Bell C. The nervous system of the human body. London: Longman, Rees, Orme, Brown, and Green; 1830: clxiii.
10. McGreevy, Joe W., Chady H. Hakim, Mark A. McIntosh, and Dongsheng Duan. “Animal Models of Duchenne Muscular Dystrophy: From Basic Mechanisms to Gene Therapy.” *Disease Models & Mechanisms* 8, no. 3 (March 1, 2015): 195.
11. McNally, Elizabeth M., et al. “The Dystrophin Glycoprotein Complex Signaling Strength and Integrity for the Sarcolemma.” *American Heart Association*, vol. 94, no. 8, 2004, pp. 1023–31, doi: 10.1161/01.RES.0000126574.61061.25.
12. Gowers WR. A manual of disease of the nervous system. London: Churchill, 1886;1:391–4.
13. Gowers WR. Pseudo-hypertrophic muscular paralysis. London: Churchill; 1879.
14. Darras BT, Urion DK, Ghosh PS. Dystrophinopathies. *GeneReviews®*. Updated Apr 26, 2018

15. Lo Mauro, Antonella, and Andrea Aliverti. “Physiology of respiratory disturbances in muscular dystrophies.” *Breathe (Sheffield, England)* vol. 12,4 (2016): 318-327. doi:10.1183/20734735.012716
16. Sheehan, Daniel W., David J. Birnkrant, Joshua O. Benditt, Michelle Eagle, Jonathan D. Finder, John Kissel, Richard M. Kravitz, et al. “Respiratory Management of the Patient with Duchenne Muscular Dystrophy.” *Pediatrics* 142, no. Supplement 2 (October 2018): S62–71.
17. Wang, Mary, David J Birnkrant, Dennis M Super, Irwin B Jacobs, and Robert C Bahler. “Progressive Left Ventricular Dysfunction and Long-Term Outcomes in Patients with Duchenne Muscular Dystrophy Receiving Cardiopulmonary Therapies.” *Open Heart* 5, no. 1 (March 2018): e000783.
18. McNally, Elizabeth M. “Cardiomyopathy in Muscular Dystrophy: When to Treat?” *JAMA Cardiology* 2, no. 2 (February 1, 2017): 199–199.
19. Farini, Andrea, Aoife Gowran, Pamela Bella, Clementina Sitzia, Alessandro Scopece, Elisa Castiglioni, Davide Rovina, et al. “Fibrosis Rescue Improves Cardiac Function in Dystrophin-Deficient Mice and Duchenne Patient–Specific Cardiomyocytes by Immunoproteasome Modulation.” *The American Journal of Pathology* 189, no. 2 (February 1, 2019): 339–53.
20. G Cheeran, Daniel, Shaida Khan, Rohan Khera, Anish Bhatt, Sonia Garg, Justin L. Grodin, Robert Morlend, et al. “Predictors of Death in Adults with

Duchenne Muscular Dystrophy–Associated Cardiomyopathy." *Journal of the American Heart Association* 6, no. 10 (October 11, 2017).

21. Van Ruiten, H.J.A., C. Marini Bettolo, T. Cheetham, M. Eagle, H. Lochmuller, V. Straub, K. Bushby, and M. Guglieri. "Why Are Some Patients with Duchenne Muscular Dystrophy Dying Young: An Analysis of Causes of Death in North East England." *European Journal of Paediatric Neurology* 20, no. 6 (November 2016): 904–9.
22. Nitahara-Kasahara, Yuko, Hiromi Hayashita-Kinoh, Tomoko Chiyo, Akiyo Nishiyama, Hironori Okada, Shin'ichi Takeda, and Takashi Okada. "Dystrophic Mdx Mice Develop Severe Cardiac and Respiratory Dysfunction Following Genetic Ablation of the Anti-Inflammatory Cytokine IL-10." *Human Molecular Genetics* 23, no. 15 (August 1, 2014): 3990–4000.
23. Rae MG, O'Malley D. Cognitive dysfunction in Duchenne muscular dystrophy: a possible role for neuromodulatory immune molecules. *J Neurophysiol*. September 1 2016; 116(3):1304-15.
24. Iyer, Vijaya. "Muscular Dystrophy | News Today." Muscular Dystrophy News, 2019, musculardystrophynews.com/breathing-problems.
25. Mavrogeni, Sophie et al. "Cardiac involvement in Duchenne and Becker muscular dystrophy." *World journal of cardiology* vol. 7,7 (2015): 410-4. doi:10.4330/wjc. v7.i7.410

26. Yotsukura M, Miyagawa M, Tsuya T, Ishihara T, Ishikawa K. Pulmonary hypertension in progressive muscular dystrophy of the Duchenne type. Jpn Circ J. 1988 Apr;52(4):321-6. doi: 10.1253/jcj.52.321. PMID: 3385914.
27. Shin, Jin-Hong et al. “Genotyping mdx, mdx3cv, and mdx4cv mice by primer competition polymerase chain reaction.” *Muscle & nerve* vol. 43,2 (2011): 283-6. doi:10.1002/mus.21873
28. “Mechanics of Breathing - Inspiration - Expiration.” *TeachMePhysiology*, 27 Apr. 2020.
29. Burns, David P et al. “Sensorimotor control of breathing in the mdx mouse model of Duchenne muscular dystrophy.” *The Journal of physiology* vol. 595,21 (2017): 6653-6672. doi:10.1113/JP274792
30. Huang, Ping et al. “Impaired respiratory function in mdx and mdx/utrn(+/-) mice.” *Muscle & nerve* vol. 43,2 (2011): 263-7. doi:10.1002/mus.21848
31. Walter, Maggie C, and Peter Reilich. “Recent developments in Duchenne muscular dystrophy: facts and numbers.” *Journal of cachexia, sarcopenia and muscle* vol. 8,5 (2017): 681-685. doi:10.1002/jcsm.12245
32. Quinlan, John G et al. “Evolution of the mdx mouse cardiomyopathy: physiological and morphological findings.” *Neuromuscular disorders : NMD* vol. 14,8-9 (2004): 491-6. doi:10.1016/j.nmd.2004.04.007
33. Gutpell, Kelly M et al. “Skeletal muscle fibrosis in the mdx/utrn+/- mouse validates its suitability as a murine model of Duchenne muscular dystrophy.” *PloS one* vol. 10,1 e0117306. 21 Jan. 2015, doi:10.1371/journal.pone.0117306

34. Ishizaki, Masatoshi et al. “Mdx respiratory impairment following fibrosis of the diaphragm.” *Neuromuscular disorders : NMD* vol. 18,4 (2008): 342-8. doi:10.1016/j.nmd.2008.02.002

35. Stevens, E D, and J A Faulkner. “The capacity of mdx mouse diaphragm muscle to do oscillatory work.” *The Journal of physiology* vol. 522 Pt 3,Pt 3 (2000): 457-66. doi:10.1111/j.1469-7793.2000.t01-3-00457.x

36. Lidov, H G. “Dystrophin in the nervous system.” *Brain pathology (Zurich, Switzerland)* vol. 6,1 (1996): 63-77. doi:10.1111/j.1750-3639.1996.tb00783.x

37. Burns, David P et al. “Inspiratory pressure-generating capacity is preserved during ventilatory and non-ventilatory behaviours in young dystrophic mdx mice despite profound diaphragm muscle weakness.” *The Journal of physiology* vol. 597,3 (2019): 831-848. doi:10.1113/JP277443

38. Mosqueira, Matias et al. “Ventilatory chemosensory drive is blunted in the mdx mouse model of Duchenne Muscular Dystrophy (DMD).” *PloS one* vol. 8,7 e69567. 29 Jul. 2013, doi:10.1371/journal.pone.0069567

39. Song, Tae-Jin et al. “Three cases of manifesting female carriers in patients with Duchenne muscular dystrophy.” *Yonsei medical journal* vol. 52,1 (2011): 192-5. doi:10.3349/ymj.2011.52.1.192